Volatile distribution in Earth's mantle heterogeneities

Mateusz M. Michailow
Department of Chemical and Geological Sciences, University of Modena and Reggio Emilia, Via G. Campi 103, 41125 Modena
DOI: 10.19276/plinius.2026.01.010

INTRODUCTION

The presence of compositional heterogeneities in the Earth's mantle has long been debated as the cause of isotopic and compositional variabilities in Mid Ocean Ridge Basalts (MORB) possibly due to assimilation of melts derived from components with lower melting temperatures than the surrounding mantle. These components are introduced into the mantle at subduction zones and are subsequently folded and stretched by mantle convective motions. The resulting heterogeneous mantle rises below Mid Ocean Ridges (MOR) and undergoes decompressional partial melting, forming magmas that carry chemical signatures of lithological heterogeneities. Magmas originated from different depths, and lithologies in the mantle are extensively mixed, hampering the possibility to recognize the geochemical signatures of single components. Regions of the MOR system where melts are created but not mixed are needed to identify these sources. This can be tested by examining ridge segments with low mantle temperatures, where reduced melting preferentially extracts low-solidus mantle domains (Brunelli et al., 2025). Analysis of volatile concentrations and isotope ratios in fresh glass samples could help understand mantle convection mechanisms and their heterogeneity.

Basaltic glasses from the Equatorial Atlantic (Eastern Romanche ridge-transform intersection, ERRTI) collected during the SMARTIES 2019 expedition (Maia et al., 2020) and dredged during previous expeditions during the PRIMAR project (Bonatti et al., 1991; 1994; Schilling et al., 1995; Gasperini et al., 1997) have been analyzed alongside a set of basaltic glasses recovered from the Vema fracture zone.

The Romanche Fracture Zone, is a major equatorial displacement of the MAR, extending from the Gulf of Guinea continental shelf, all the way across the Equatorial Atlantic Ocean, to a section of the North Brazilian Ridge. The lens-shaped transform domain is composed of a wide-ranging (~ 100 km), extremely deformed, multi-fault system, with an estimated offset of ~ 950 km, one of the longest offsets worldwide (Bonatti et al., 1994, 1996; 2001; Bonatti, 1996; Ligi et al., 2002; 2022). The ERRTI area is characterized by a predominance of mantle-derived rocks (mainly melt-impregnated peridotites), and a very scarce occurrence of basaltic rocks. This prominent shortage of basaltic crust could attest for a remarkable reduction of mantle partial melting. The prominent "cold edge effect" of this area lowers the degree of melting, allowing the extraction of melts from the low solidus heterogeneities present in the mantle (Bonatti et al., 1994, 1996; Bonatti, 1996; Ligi et al., 2002; Brunelli et al., 2025).

As illustrated by Brunelli et al. (2025), basaltic glasses from the ERRTI display a clear enrichment in alkalis and other incompatible elements. Their compositions span the full tholeiitic range, clustering at its alkali-rich end, and reaching the alkaline field, including both silica-saturated and silica-undersaturated terms. Basaltic glass fragments from the Romanche ERRTI exhibit isotopic compositions that extend beyond the typical range of MORBs (represented here by the more homogeneous Vema samples), overlapping with much of the global Ocean Island Basalt (OIB) field. Their Sr, Nd, Pb, and Hf isotope ratios show remarkable variability: $^{87}Sr/^{86}Sr$ from 0.702398 to 0.703758, $^{143}Nd/^{144}Nd$ from 0.512752 to 0.513225, $^{206}Pb/^{204}Pb$ from 18.503 to 19.700, and $^{176}Hf/^{177}Hf$ from 0.282674 to 0.283443. This range exceeds the full isotopic diversity observed along the Mid-Atlantic Ridge approaching the extent of the hotspot variability (Brunelli et al., 2025).

This study determines the volatile absolute concentrations and isotopic compositions of these glasses, comparing them with their major, trace, and radiogenic compositions. An extensive study of dissolved sulfur alongside the study of immiscible sulfide phases in the glass matrix helps understanding the behavior of sulfur during mantle melting in a low thermal region such as ERRTI and identify possible mixing-induced geochemical signatures. In addition, boron isotopes are used to exclude late hydrothermal alteration processes. Volatile abundances, sulfur and boron isotopes and sulfide inclusions analyses have been carried out at the Woods Hole Oceanographic Institution using Secondary Ion Mass Spectrometry (SIMS).

METHODS

Glass samples were examined using the SIMS for volatile concentrations and isotopic compositions using the CAMECA IMS 1280, a double-focusing mass spectrometer with high mass resolution power (MRP).

Glass fragments were embedded in epoxy resin and polished, placed in an indium mount, dried in a vacuum oven at 50°C for 48h, and eventually gold coated. Mounts were degassed in the IMS 1280 airlock at pressures of ~ 10^{-9} torr for 48h, then placed into the sample chamber at ~ 3.6 x 10^{-9} torr.

Sulfur Isotope analysis

Sulfur $^{34}S/^{32}S$ isotope ratios were measured using both mono- and multi-collection approaches. Measurements employed a primary Cs^+ ion beam.

In monocollection mode, two species, ^{32}S and ^{34}S, were measured for S isotope analyses with a MRP between 4998 and 6743. The primary ion beam (700-750 pA) was rastered over an area of 30 × 30 µm. Each measurement consisted of 40 cycles, on 3 different spots. The analysis consisted of a pre-sputtering time of 150 s, a cycle time of 2.96 s for ^{32}S and 8.00 s for ^{34}S, with a waiting time of 2.00 s.

In multicollection mode, both sulfur content and $^{34}S/^{32}S$ isotope ratios were measured in the same analytical session, greatly reducing analysis time. ^{32}S, ^{34}S, and ^{30}Si were measured with a MRP of 4998. All the species were measured on four EM detectors positioned at appropriate species-specific positions. The primary ion beam (300 pA) was rastered over an area of 15 × 15 µm. Each sample was analyzed on 2 to 3 different spots, and each measurement consisted of 80 cycles. The analysis consisted in a pre-sputtering time of 240 s, a cycle time of 4 s for all species, with a waiting time of 0.4 s. Each analysis chain contained known standard measurements to assess backgrounds, accuracy, and reproducibility. All the measurements have been carried out with a semi-automatic mass calibration and beam centering.

A total of 25 pre-selected sulfide droplets were analyzed for $\delta^{34}S$ in polished, gold-coated glass fragments. Sulfur isotopes (^{32}S and ^{34}S) were measured using a multi-collector SIMS setup with a 150 pA Cs^+ primary ion beam and four Faraday detectors. The two species, ^{32}S and ^{34}S, were measured at an MRP of 4998. The Cs^+ beam was rastered across a 5 × 5 µm area. Each analysis included 40 cycles, consisting of a 180 s pre-sputtering time, a cycle time of 8 s for both ^{32}S and ^{34}S, and a 0.40 s waiting time. Sulfides consist of intergrown pyrrhotite (Po), chalcopyrite (Cp), and pentlandite (Pn), with analysis spots sampling all phases in varying proportions. The reported $\delta^{34}S$ values were therefore corrected to account for sulfide heterogeneity, following SEM-EDS compositional analyses identifying sulfide phases and estimating their relative proportions on the exposed surface.

Volatile content analysis

Volatile content analysis was performed using a 1 nA primary Cs^+ ion beam, accelerated at a voltage of 20 kV. The primary beam was tuned using an Al-Cu tuning grid and $^{27}Al^{16}O$ signal for peak calibration. An electron gun was used to flood the Cs beam spot area with a cloud of charge compensating electrons, to prevent positive electrostatic charge build-up during sputtering. Secondary Ions (^{12}C, $^{16}O^1H$, ^{19}F, ^{30}Si, ^{32}S and ^{35}Cl) were measured using a single electron multiplier, and MRP of 6743 to overcome mass isobaric interferences. Each glass sample was analyzed on 3 different spots, with 5 cycles per measurement. All the measurements have been carried out with a semi-automatic mass calibration and beam centering, and contained known standard measurements to assess background, accuracy, and reproducibility.

Boron Isotope analysis

Boron concentration and the $^{11}B/^{10}B$ isotope ratio were measured both in the same analytical session employing a multicollection mode approach. ^{11}B and ^{10}B along the ^{30}Si were measured with a MRP of 2427. Boron isotopes were measured on two different EM detectors positioned at appropriate species-specific positions, while Si was measured on a faraday cup detector. A primary O^{2-} ion beam of 40 nA was rastered over an area of 20 × 20 µm. Each sample was analyzed on 3 different spots, and each measurement consisted of 40 cycles. The analysis consisted in a pre-sputtering time of 300 s, a cycle time of 14.96 s for ^{11}B and ^{10}B, ^{30}Si was measured with a cycle time of 2.96 s; the waiting time was set to 3.04 s for all the measured species.

RESULTS

Sulfur isotopic composition

The isotopic composition of ERRTI glasses display $\delta^{34}S$ values that vary from -4.57‰ to +6.94‰ (mean value of +1.64 ± 4.57‰, 2SD, n = 115). Analyzed MORBs have mostly positive $\delta^{34}S$ with the exception of 14 samples that exhibit negative $\delta^{34}S$ values that range between -0.21 ± 0.71‰ and -4.57 ± 1.21‰. Most of the samples show a $\delta^{34}S$ variability higher than average MORBs (-0.9 ± 0.50‰; Labidi et al., 2012), and some of the samples show deviations towards more ^{34}S enriched delta values reaching up to +6.94 ± 1.95‰. A total of 15 samples have $\delta^{34}S$ values between +3.01 ± 2.64‰ and +6.94 ± 1.95‰, values higher than typical MORBs $\delta^{34}S$ values. Vema samples show $\delta^{34}S$ between -2.86 and +4.90‰ (mean value of -0.03 ± 3.37‰, 2SD, n = 32), a distribution compatible with that of global MORBs. Compared to Vema, ERRTI samples show a noticeable shift towards ^{34}S enriched values.

The isotopic composition of sulfide droplets presents a systematic shift with respect to host glasses.

They present lower values spanning to markedly negative $\delta^{34}S$ with no apparent correlation with the total S content. Host glasses have $\delta^{34}S$ values from +0.95‰ to +6.89‰ (mean value of +1.89 ± 5.25‰, 2SD). The difference between $\delta^{34}S$ of sulfdies and host-glass ($\Delta^{34}S_{sulfide\text{-}glass}$) is between -8.53 and +2.04‰.

Volatile concentrations

Measured volatile concentration in ERRTI glasses vary significantly: from 78.7 to 261.3 ppm for CO_2 (average 163.2 ± 78.3, 2SD), from 0.15 to 1.57 wt.% for H_2O (average 0.58 ± 0.56, 2SD), from 100.9 to 1199 ppm for F (average 383.1 ± 411.9, 2SD), from 584.8 to 2112 ppm for S (average 1016 ± 508, 2SD) and from 41.3 to 1016 ppm for Cl (average 235.1 ± 378.9, 2SD). Vema concentrations are respectively from 43.7 to 5205 ppm for CO_2 (average 281.3 ± 136.6, 2SD), from 0.20 to 0.47 wt.% for H_2O (average 0.27 ± 0.10, 2SD), from 130.04 to 278.9 ppm for F (average 183.2 ± 57.8, 2SD), from 933.1 to 1356.8 ppm for S (average 1094 ± 168.9, 2SD) and from 4.03 to 125.6 ppm for Cl (average 20.6 ± 30.98, 2SD).

Boron isotopic composition

The boron concentration of the analyzed ERRTI glasses varies between 0.39 and 3.47 ppm with a mean value of 1.43 ± 1.53 ppm (2SD, n = 29). The boron isotopic composition of the analyzed glass fragments shows a $\delta^{11}B$ range between -1.28 and -8.52‰ with a mean value of -4.74 ± 3.81‰ (2SD, n = 29). Most of our B dataset fits within the uncontaminated MORB range with values between 0.39 ± 0.018 and 2.49 ± 0.096 ppm (n = 27). The boron isotopic distribution of ERRTI lavas similarly spans the global $\delta^{11}B$ MORB array, although with an average ERRTI $\delta^{11}B$ value (-4.74 ± 3.81‰) slightly higher than the uncontaminated MORB $\delta^{11}B$ of -7.1 ± 0.9‰ (Marschall et al., 2017).

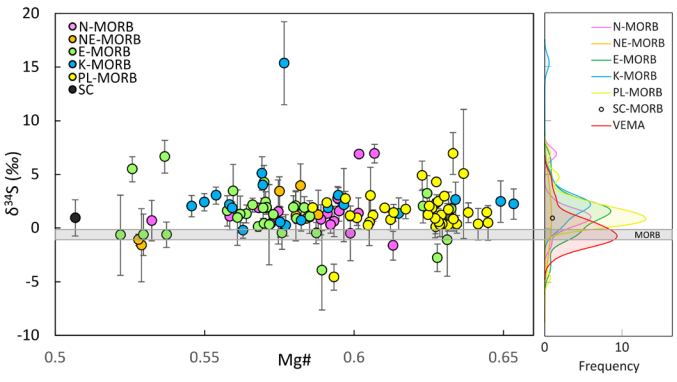

Figure 1 Sulfur isotopic variability of the measured glass fragments for ERRTI and Vema samples. Frequency distribution of $\delta^{34}S$ values relative to the average MORB $\delta^{34}S$ value of -0.9 ± 0.50‰ (grey area; Labidi et al., 2012) shows that all ERRTI groups present a significant tail toward high ^{34}S values compared to MORBs, with E-MORBs (green) and K-MORBs (blue) having the highest $\delta^{34}S$ shift than N-MORBs (purple) and PL-MORBs (yellow). Vema samples (red) show a distribution coherent with the average MORB value.

DISCUSSION

Shape, texture, and composition of the observed sulfide droplets confirm their magmatic origin as an immiscible sulfide liquid. The observed Cu–Ni–Fe-rich sulfides in ERRTI glasses formed through sulfur immiscibility from a sulfide-saturated melt crystallizing between 1100–900°C. Limited dissolution features suggest rapid quenching preserved these inclusions. The ^{34}S enrichment in glasses (Fig. 1) cannot be explained by degassing or sulfide separation at typical oxidizing MORB conditions. Both will require unrealistic degrees of S loss (more than 90%), low temperatures (< 700°C) and oxidizing conditions (ΔFMQ > 1, outside of the MORB range) not observed in the sampled suite (-0.9 > ΔFMQ > +0.82), indicating that sulfides and host glasses derive from distinct $\delta^{34}S$ sources. An average $\alpha_{sulfide\text{-}melt}$ of 0.99702 ± 0.0057 between ^{34}S depleted sulfides and glasses with atypical isotopic ^{34}S enrichments (Fig. 2) points to different isotopic origins for sulfides and silicate glass. The ^{34}S enrichment across samples might reflect assimilation of ^{34}S-rich recycled sulfur, rather than magmatic fractionation or crustal contamination. The large sulfur isotopic variability in both host-glass and sulfides might indicate that the mantle source is unlikely to be a typical depleted mantle reservoir associated with normal MORB formation.

The Earth's mantle contains recycled crustal sulfur, with extremely variable $\delta^{34}S$ values (Burness et al., 2021), in stark contrast to the mantle's relatively homogeneous signature, pointing to the incorporation of subducted

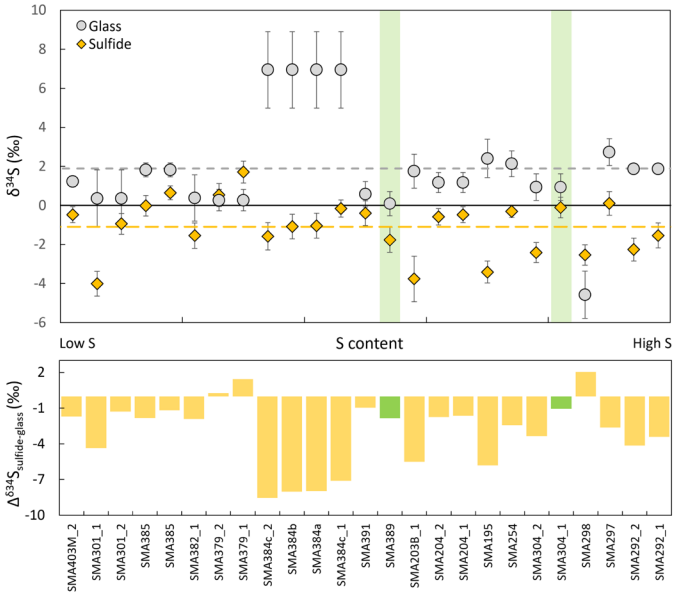

Figure 2 Upper panel: Sulfur isotopic variability in measured ERRTI sulfide droplets (yellow) and host glasses (grey) ordered according to their S content. The yellow dashed line represents the average $\delta^{34}S$ sulfide value (-1.11 ± 2.79‰ 2SD) for all the measured sulfides. The grey dashed line is the average $\delta^{34}S$ value (+1.89 ± 5.25‰ 2SD) for all the measured glasses. Sulfide values are corrected taking into account sulfide phase heterogeneity. Lower panel: the $\Delta^{34}S_{sulfide\text{-}glass}$ for the analyzed sulfide-glass couples. All the measured sulfides are hosted in PL-MORB glass samples except two (SMA379_1 and SMA384c_1) hosted in E-MORB samples (in green) hosting visible sulfide droplets. There is no correlation between the observed $\Delta^{34}S_{sulfide\text{-}glass}$ and the S content of the glass.

components (Farquhar et al., 2002; Delavault et al., 2016; Burness et al., 2021). All ERRTI lavas display a ^{34}S enrichment irrespective of compositional group that cannot be explained by secondary processes. This enrichment likely reflects the incorporation of a component with $\delta^{34}S$ between +8‰ and +20‰ during magma evolution, possibly derived from recycled sulfide minerals, ancient sedimentary sulfur, or a HIMU-like source with positive $\delta^{34}S$ (Fig. 3). The analyzed sulfides might be remnants of a sulfide saturated melt formed from the melting of a recycled HIMU-like component with negative $\delta^{34}S$ composition. Partial melting of HIMU-type recycled (meta-gabbroic) pyroxenites relic of ancient oceanic lithosphere (Brunelli et al., 2025) may generate a S-saturated melt because of the low sulfur solubility during the melting of mafic pyroxenites, promoting the segregation of immiscible sulfide melts (Montanini et al., 2010) before the onset of partial melting of the host peridotitic mantle. Once formed, sulfide melts remain trapped within the silicate matrix. Their preservation during subsequent mixing with other components (*e.g.*, DMM, EM-II) attests to the fact that these melts never evolved to oxidizing conditions and therefore maintained low sulfur content at sulfide saturation values.

The ^{34}S depleted isotopic composition of the sulfide droplets might therefore represent the isotopic signature of preserved ancient highly $\delta^{34}S$ negative sulfides that initially formed within the recycled altered oceanic lithosphere.

SIMS analysis of basaltic glass fragments from the Vema and ERRTI areas suggests that variations in volatile concentrations (CO_2, H_2O, S, Cl, F) are primarily a result of differences in mantle sources rather than processes like fractional crystallization or degassing. Findings indicate limited degassing, particularly for H_2O, Cl, and F, and point to enriched and heterogeneous mantle sources that might have been influenced by recycled oceanic crustal components. The poorly mixed ERRTI basaltic glasses, compared with the reference homogeneous MORB glasses from the Vema fracture zone, show a strong increase in the concentration and variability of the volatile species. Higher concentrations and deviations from the observed global MORB trend for volatile-trace element pairs (Fig. 4), together with radiogenic isotopic compositions of these glasses, confirm possible recycling of subducted components and the presence of both volatile rich and volatile depleted enriched MORB melts.

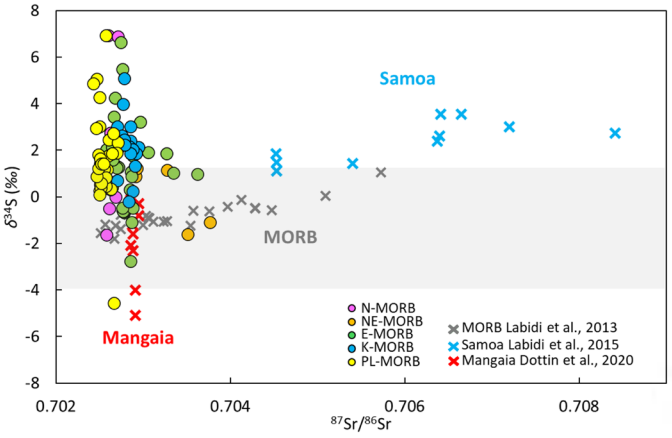

Figure 3 *$\delta^{34}S$ vs $^{87}Sr/^{86}Sr$ for the analyzed ERRTI glasses compared to literature data for Mangaia (red crosses, Dottin et al., 2020), Samoa (blues crosses, Workman et al., 2006; Labidi et al., 2015) and MORB (green crosses, Labidi et al., 2013). The grey area corresponds to the $\delta^{34}S$ values of measured sulfide droplets (only one sulfide has a $\delta^{34}S$ of 1.71‰, all other sulfides vary between -4.01‰ and 0.64‰). ERRTI glasses show a shift towards more positive $\delta^{34}S$ values for the same $^{87}Sr/^{86}Sr$.*

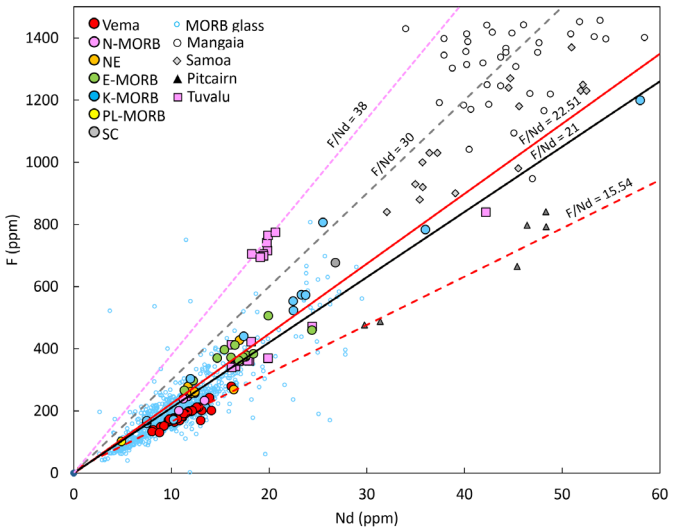

Figure 4 *F and Nd concentrations of Vema and ERRTI glass samples compared to the global MORB glass dataset (Le Voyer et al., 2019), olivine hosted melt inclusions from the equatorial MAR (Le Voyer et al., 2017), Mangaia (Cabral et al., 2014), Pitcairn and Samoa (Kendrick et al., 2017) and Tuvalu (Jackson et al., 2015). Vema samples are correlated for an F/Nd of 15.54 remarkably similar to the DMM F/Nd value of 15.5 ± 4.8 (Salters & Stracke, 2004). ERRTI samples follow an average F/Nd value of 22.51, slightly higher than the F/Nd of 21 for MORBs. Mangaia samples follow an average F/Nd of 30 while the mildly HIMU Tuvalu samples and F/Nd of 38. The most enriched ERRTI E- and K-MORBs follow an F/Nd of 25–26 with one exceptionally high K-MORB sample with an F/Nd of 31.59. The most volatile-enriched ERRTI samples show an offset indicative of HIMU or EM-II influence in the source region (figure modified after Cabral et al., 2014 and Jackson et al., 2015).*

The boron composition of most of the analyzed glasses fall within the range of uncontaminated MORBs (0.4-2.5 ppm B; $\delta^{11}B$ = -7.1 ± 0.9‰; Marschall et al., 2017), indicating negligible seawater or hydrothermal alteration. Variations in B/Ce (0.047–0.092) correlate with radiogenic isotope systematics and trace element indicators, suggesting that the observed heterogeneity reflects compositional unmixing of variably enriched and depleted mantle sources. The HIMU-like K-MORBs display the lowest B/Ce ratios, consistent with a dehydrated, recycled oceanic crustal component. Slight $\delta^{11}B$ enrichment relative to the MORB average likely records residual effects of subduction-related dehydration during mantle re-incorporation. These results demonstrate that boron isotopes and content in ERRTI lavas preserve signatures of ancient subducted lithologies (Fig. 5) and provide new constraints on volatile recycling in heterogeneous mantle domains.

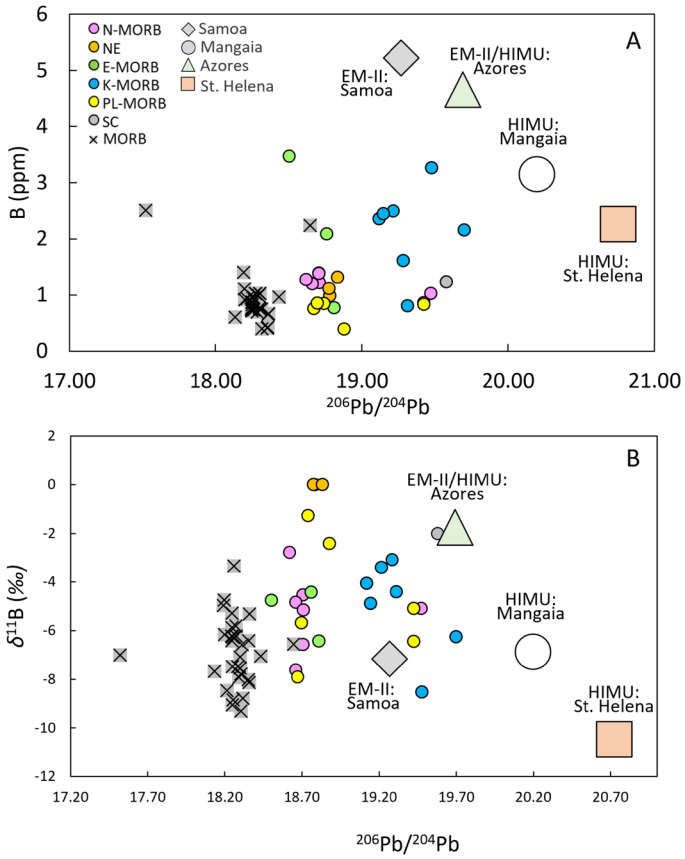

Figure 5 a) *B content vs $^{206}Pb/^{204}Pb$ of the analyzed ERRTI glasses compared to global MORB (Marschall et al., 2017), HIMU-type lavas (Mangaia average B value from Cabral et al., 2014; Azores average B value from Turner et al., 2007; Genske & Turner, 2014; St. Helena average B value from Chaussidon & Marty, 1995; Walowski et al., 2021; Average $^{206}Pb/^{204}Pb$ values from GEOROC), and EM-II type lavas (Samoa; average B and $^{206}Pb/^{204}Pb$ from GEOROC);* ***b)*** *$\delta^{11}B$ vs $^{206}Pb/^{204}Pb$ of the analyzed ERRTI glasses compared to global MORBs (Marschall et al., 2017), HIMU-type lavas (Mangaia average $\delta^{11}B$ value from unpublished data Marschall & Jackson, 2020; Azores average $\delta^{11}B$ value from Turner et al., 2007; Genske & Turner, 2014; St. Helena average $\delta^{11}B$ value from Chaussidon & Marty, 1995; Walowski et al., 2021), and EM-II type lavas (Samoa; average $\delta^{11}B$ value from unpublished data Marschall & Jackson, 2020 and $^{206}Pb/^{204}Pb$ from GEOROC). Average $^{206}Pb/^{204}Pb$ values from GEOROC.*

CONCLUSIONS

In conclusion, the SIMS analyses on submarine basaltic glasses, sampled from the Vema and the ERRTI in the Equatorial Atlantic, suggests that:

1. Fractional crystallization and degassing play a minor role in H_2O, Cl and F distribution in Equatorial Mid Atlantic Ridge MORBs. High Cl, F, H_2O, and S concentrations observed in enriched mantle components are representative of ancient enriched recycled lithological heterogeneity.

2. Sulfur isotope variability points to a heterogeneous mantle source containing recycled sulfur components. The occurrence of relatively ^{34}S-enriched glasses alongside ^{34}S-depleted sulfide droplets implies incomplete mixing of isotopically different sulfur reservoirs during melt formation and ascent under low-temperature melting conditions, consistent with the preservation of recycled sulfur signatures in the mantle.

3. Slightly higher $\delta^{11}B$ values relative to average MORB (mean shift of +2.4‰) suggest partial retention of subduction-related isotopic signatures in mantle sources beneath the Equatorial MAR. Combined B-radiogenic isotope systematics reveal efficient unmixing of enriched (HIMU and EM-II) and depleted mantle domains under a cold thermal regime that limited melt homogenization.

REFERENCES

Bonatti, E. (1996) - Anomalous opening of the Equatorial Atlantic due to an equatorial mantle thermal minimum. Earth. Planet. Sc. Lett., 143, 147–160.

Bonatti, E., Brunelli, D., Fabretti, P., Ligi, M., Asunta Portaro, R., Seyler, M. (2001) - Steady-state creation of crust-free lithosphere at cold spots in mid-ocean ridges. Geol., 29, 979.

Bonatti, E., Ligi, M., Carrara, G., Gasperini, L., Turko, N., Perfiliev, S., Peyve, A., Sciuto, P.F. (1996) - Diffuse impact of the Mid-Atlantic Ridge with the Romanche transform: an ultracold ridge-transform intersection. J. Geophys. Res., 101, 8043–8054.

Bonatti, E., Ligi, M., Gasperini, L., Peyve, A., Raznitsin, Y., Chen, Y.J. (1994) - Transform migration and vertical tectonics at the Romanche fracture zone, equatorial Atlantic. J. Geophys. Res., 99, 21779–21802.

Bonatti, E., Raznitsin, Y., Bortoluzzi, G., Boudillon, F., De Alteriis, G., Gasperini, L., Gasperini, M., Giaquinto, G., Ligi, M., Sacchi, M., Skolotnev, S., Trofimov, V., Turco, N., Zacharov, M., Auzende, J.M., Mamaloukis Frangoulis, V., Searle, R. (1991) - Geological studies of the eastern part of the Romanche transform (equatorial Atlantic): A first report. Giorn. Geol., 53, 31–48.

Burness, S., Thomassot, E., Smart, K.A., Tappe, S. (2021) - Sulphur isotopes ($\delta^{34}S$ and $\Delta^{33}S$) in sulphides from cratonic mantle eclogites: A glimpse of volatile cycling in ancient subduction zones. Earth. Planet. Sc. Lett., 572, 117118.

Brunelli, D., Verhoest, L., Ligi, M., Hemond, C., Maia, M., Soltanmohammadi, A., Lugli, F., Nonnotte, P., Cipriani, A. (2025) - Large melt diversity at a mid-ocean ridge thermal low. Sci. Adv., 11, eadv4654.

Cabral, R.A., Jackson, M.G., Koga, K.T., Rose-Koga, E.F., Hauri, E.H., Whitehouse, M.J., Price, A.A., Day, J.M.D., Shimizu, N., Kelley, K.A. (2014) - Volatile cycling of H_2O, CO_2, F, and Cl in the HIMU mantle: A new window provided by melt inclusions from oceanic hot spot lavas at Mangaia, Cook Islands. Geochem. Geophys. Geosyst., 15, 4445–4467.

Chaussidon, M. & Marty, B. (1995) - Primitive Boron Isotope Composition of the Mantle. Science, 269, 383–386.

Delavault, H., Chauvel, C., Thomassot, E., Devey, C.W., Dazas, B. (2016) - Sulfur and lead isotopic evidence of relic Archean sediments in the Pitcairn mantle plume. Proc. Natl. Acad. Sci. U.S.A., 113, 12952–12956.

Dottin, J.W., Labidi, J., Jackson, M.G., Woodhead, J., Farquhar, J. (2020) - Isotopic Evidence for Multiple Recycled Sulfur Reservoirs in the Mangaia Mantle Plume. Geochem. Geoph. Geosys., 21, e2020GC009081.

Farquhar, J., Wing B.A., McKeegan, K.D., Harris, J.W., Cartigny, P., Thiemens, M.H. (2002) - Mass-Independent Sulfur of Inclusions in Diamond and Sulfur Recycling on Early Earth. Science, 298, 2369–2372.

Gasperini, L., Bonatti, E., Brunelli, D., Carrara, G., Cipriani, A., Fabretti, P., Gilod, D., Ligi, M., Peyve, A., Skolotnev, S., Susini, S., Tartarotti, P., Turko, N. (1997) - New data on the geology of the Romanche F.Z., equatorial Atlantic: PRIMAR-96 cruise report. Giorn. Geol., 59.

Genske, F.S., Turner, S.P., Beier, C., Chu, M.F., Tonarini, S., Pearson, N.J., Haase, K.M. (2014) - Lithium and boron isotope systematics in lavas from the Azores islands reveal crustal assimilation. Chem. Geol., 373, 27–36.

Jackson, M.G., Koga, K.T., Price, A., Konter, J.G., Koppers, A.a.P., Finlayson, V.A., Konrad, K., Hauri, E.H., Kylander-Clark, A., Kelley, K.A., Kendrick, M.A. (2015) - Deeply dredged submarine HIMU glasses from the Tuvalu Islands, Polynesia: Implications for volatile budgets of recycled oceanic crust. Geochem. Geophys. Geosyst., 16, 3210–3234.

Kendrick, M.A., Hémond, C., Kamenetsky, V.S., Danyushevsky, L., Devey, C.W., Rodemann, T., Jackson, M.G., Perfit, M.R. (2017) - Seawater cycled throughout Earth's mantle in partially serpentinized lithosphere. Nature Geosci., 10, 222–228.

Labidi, J., Cartigny, P., Birck, J.L., Assayag, N., Bourrand, J.J. (2012) - Determination of multiple sulfur isotopes in glasses: A reappraisal of the MORB $\delta^{34}S$. Chem. Geol., 334, 189–198.

Labidi, J., Cartigny, P., Jackson, M.G. (2015) - Multiple sulfur isotope composition of oxidized Samoan melts and the implications of a sulfur isotope 'mantle array' in chemical geodynamics. Earth Planet Sc. Lett., 417, 28–39.

Labidi, J., Cartigny, P., Moreira, M. (2013) - Non-chondritic sulphur isotope composition of the terrestrial mantle. Nature, 501, 208–211.

Le Voyer, M., Hauri, E.H., Cottrell, E., Kelley, K.A., Salters, V.J.M., Langmuir, C.H., Hilton, D.R., Barry, P.H., Füri, E. (2019) - Carbon Fluxes and Primary Magma CO_2 Contents Along the Global Mid-Ocean Ridge System. Geochem. Geophys. Geosyst., 20, 1387–1424.

Le Voyer, M., Kelley, K.A., Cottrell, E., Hauri, E.H. (2017) - Heterogeneity in mantle carbon content from CO_2-undersaturated basalts. Nat. Commun., 8, 14062.

Ligi, M., Bonatti, E., Gasperini, L., Poliakov, A.N.B. (2002) - Oceanic broad multifault transform plate boundaries. Geol., 30, 11.

Ligi, M., Cuffaro, M., Muccini, F., Bonatti, E. (2022) - Generation and evolution of the oceanic lithosphere in the North Atlantic. Riv. Nuovo Cim., 45, 587–659.

Maia M., Brunelli, D., SMARTIES Cruise Scientific Party (2020) - The Eastern Romanche ridge-transform intersection (Equatorial Atlantic): slow spreading under extreme low mantle temperatures. Preliminary results of the SMARTIES cruise, oral.

Marschall, H.R., Wanless, V.D., Shimizu, N., Pogge von Strandmann, P.A.E., Elliott, T., Monteleone, B.D. (2017) - The boron and lithium isotopic composition of mid-ocean ridge basalts and the mantle. Geochim. Cosmochim. Ac., 207, 102–138.

Marschall, H. & Jackson, M. (2020) - Low recycling efficiency of boron into the deep mantle, EGU General Assembly 2020, Online, 4–8 May, EGU2020-10054.

Montanini, A., Tribuzio, R., Bersani, D. (2010) - Insights into the origin of mantle graphite and sulphides in garnet pyroxenites from the External Liguride peridotites (Northern Apennine, Italy). SP, 337, 87–105.

Salters, V.J.M. & Stracke, A. (2004) - Composition of the depleted mantle. Geochem. Geophys. Geosyst., 5, 2003GC000597.

Schilling, J.G.G., Ruppel, C., Davis, A.N.N., McCully, B., Tighe, S.A.A., Kingsley, R.H., Lin, J. (1995) - Thermal structure of the mantle beneath the equatorial Mid-Atlantic Ridge: Inferences from the spatial variation of dredged basalt glass compositions. J. Geophys. Res., 100, 10057–10076.

Turner, S., Tonarini, S., Bindeman, I., Leeman, W.P., Schaefer B. F. (2007) - Boron and oxygen isotope evidence for recycling of subducted components over the past 2.5 Gyr. Nature, 447, 702–705.

Walowski, K.J., Kirstein, L.A., De Hoog, J.C.M., Elliott, T., Savov, I.P., Jones, R.E., Eimf (2021) - Boron recycling in the mantle: Evidence from a global comparison of ocean island basalts. Geochim. Cosmochim. Ac., 302, 83–100.

Workman, R.K., Hauri, E., Hart, S.R., Wang, J., Blusztajn, J. (2006) - Volatile and trace elements in basaltic glasses from Samoa: Implications for water distribution in the mantle. Earth Planet Sc. Lett., 241, 932–951.